II. THEORY OF PRECIPITATION

II.A. Steps in Precipitation Reactions

The precipitation is a complex process of even an ionic salt. Even though precipitation is a fundamental chemical operation for both separation and purification it is not well understood. All too frequently precipitation only gives the desired result if certain well-established procedures are rigidly adhered to even though, in far too many cases, the basis of these procedures have evolved empirically and are, at best, poorly understood.

The simplest case is precipitation from a supersaturated solution which involves the formation of a new solid phase from solution; purification of sugar is an example of this. It is convenient to establish the following steps in this process: nucleation, growth, ripening and aging. In practice, these are not distinct since two, or even all, of the steps may overlap in time.

The next complexity in precipitation is illustrated by the mixing of two chemical solutions to form an insoluble salt. For example, the addition of barium chloride to sodium sulfate can produce insoluble barium sulfate:

$$BaCl_2 + Na_2SO_4 \rightarrow BaSO_{4_s} + 2NaCl$$

The precipitation of $BaSO_4$ by the above equation is more complex than from a supersaturated solution of just barium sulfate since concentrations are changing with time during the reaction.

II.A.1. Crystallization from a Homogeneous Solution without Reaction

Crystallization is an old process, dating at least to 1500 BC for the production of alum (II.1). However, the science describing the process is a recent development. Today this process has become quite sophisticated as is illustrated by the figure reproduced from reference II.1.

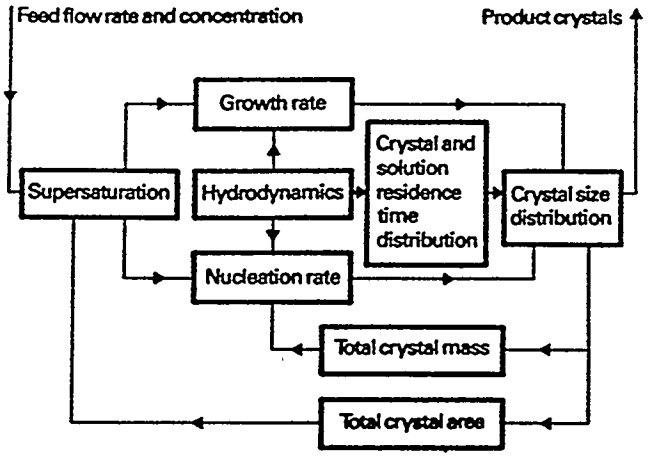

Figure II.1. Interactions within a crystallizer (reference II.1).

The kinetic description of crystal production is analogous to that of the Anderson-Schulz-Flory (ASF) treatment of Fischer-Tropsch Synthesis.

Rousseau (II.2) summarized the development of the equations to describe the size distribution of product crystals.

"We can derive equations describing the size distribution of product crystals with the following definitions and restrictions:

- The number of crystals is a balanceable quantity.

- A population density function is defined so that n(L)dL is the number of crystals in the size range L to L + dL per unit volume magma or clear liquor. We assume the function to be continuous.
- Crystal growth rate is defined as the rate of change in characteristic crystal dimension, i.e., G = dL/dt.
- The rate at which crystals grow into the size range L to L + dL is n(L)G(L).
- The rate at which crystals grow out of the size range L to L + dL is n(L + dL)G(L +dL).
- Nucleation rate, B°, is defined as the rate at which new crystals are formed in the crystallizer."

"With these definitions, the population balance on a perfectly mixed crystallizer can be written as:

$$V\left(\frac{\partial n}{\partial t} + \frac{\partial nG}{\partial L}\right) + n\,\frac{\partial V}{\partial t} + Q_o n = Q_i n_i \qquad \text{[II.1]}$$

where Q_o is the magma flow rate out of the crystallizer. Let us further assume that the magna volume, V, is constant and perfectly mixed (so that a single residence time, τ, can be used for all crystals and liquor), and if the feed to the crystallizer is clear, the population balance may be written as:

$$\frac{\partial n}{\partial t} + \frac{\partial (nG)}{\partial L} + \frac{n}{\tau} = 0 \qquad \text{[II.2]}$$

Now assuming steady-state behavior and growth that is independent of crystal size, the population density function can be written as:

$$n=n^o \exp(-L/G\tau) \qquad \text{[III.2a]}$$

where n° is the population density of zero-size crystals, often referred to as nuclei population density."

"Under steady-state conditions in a perfectly mixed crystallizer the total number production rate of crystals is identical to the nucleation rate. Accordingly:

$$B^o = \frac{1}{\tau}\int_0^\infty ndL = n^o G_\tau \qquad \text{[II.3]}$$

"Analysis of the last two equations shows that we can use a single experiment to obtain growth and nucleation rates at a single set of conditions. Figure II.2 shows a plot of typical population-density data obtained from a crystallizer meeting the assumptions stated above. The slope of these data may be used to obtain the

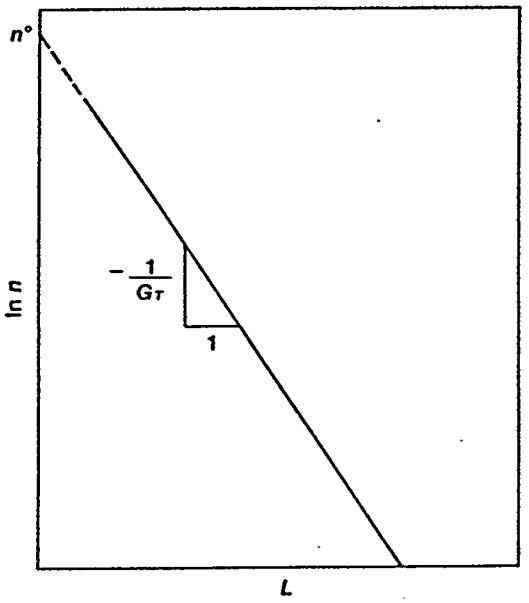

Figure II.2. Ideal exponential crystal size distribution from perfectly mixed crystallizer (reference II.2).

growth rate while the intercept gives nucleation rate. The perfectly mixed crystallizer is often used to obtain kinetic data for crystallizer design or analysis. Typically, a series

of experiments is conducted at various conditions to give growth and nucleation kinetics that may be correlated with system variables. Correlations for nucleation rate are usually in the form of power law expressions such as:

$$B^o = k_N(T,rpm)G^i M_T{}^j \qquad \text{[II.4]}$$

where i, j and k_N are system-dependent parameters and M_T is the mass of crystals per unit volume (magma density). The expression for nucleation rate kinetics usually contains the growth rate to eliminate the necessity of knowing system supersaturation, a quantity that is often difficult to measure.

The perfectly mixed crystallizer restricts the degree to which characteristics of a crystal size distribution may be varied. Such distributions have the following characteristics:

1. The dominant crystal size, that is, the mode of the mass distribution function, is $L_D = 3G_T$.
2. The coefficient of variation of the population density function is 50%; such a distribution is usually too wide for commercial products.
3. The magma density (mass of crystals per unit volume of slurry or liquor) may be obtained from the third moment of the population density function:

$$M_T = 6\rho k_v n^o (G_\tau)^4 \qquad \text{[II.5]}$$

where ρ is crystal density and k_v is the volume shape factor. Although magma density is a function of the kinetic parameters n° and G, it can be measured independently of

crystal size distribution and, where possible, it should be used as a constraint in evaluating nucleation and growth rates.

4. A pair of kinetic parameters, one for nucleation rate and another for growth rate, describe crystal size distribution for a given set of crystallizer conditions. Furthermore, one cannot vary one of the kinetic parameters without changing the other.

Experimental data for the crystal size distribution of calcium oxalate shows excellent agreement with the predicted distribution.

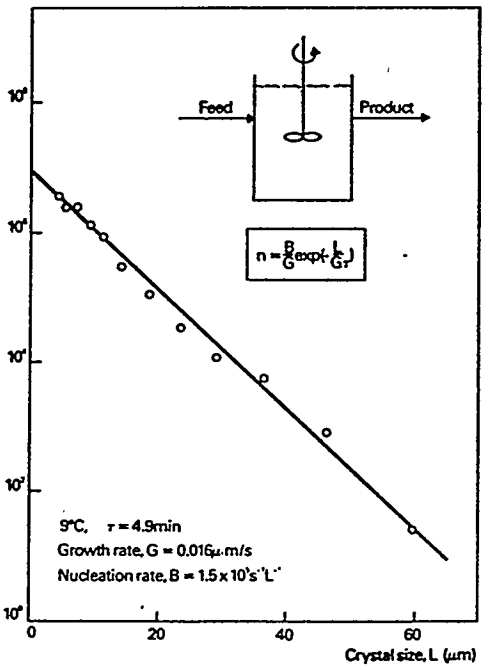

Figure II.3. Steady state crystal size distribution of calcium oxalate in a continuous mixed-suspension mixed-product removal (MSMPR) crystallizer (9°C, mean residence time (τ) = 4.9 min) (reference II.3).

The similarity between the curve in Figure II.3 (Ref. II.3) and a typical ASF is obvious in Figure II.4 (Ref. II.4). The analogy may even be carried further.

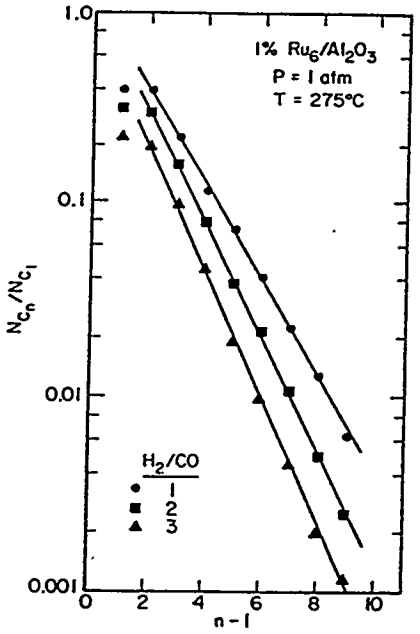

Figure II.4. Plots of log (N_{C_n}/N_{C_1}) versus (n-1) for different H_2/CO feed ratios (reference II.4).

Crystal size distributions produced in perfectly mixed crystallizers are highly constrained. When a system is operating in a high-yield mode, where no appreciable supersaturation remains in the effluent liquor, the process is even more severely constrained. In such circumstances, for example, fixing feed concentration and crystallizer conditions determine magma density.

Much of this inflexibility can be lessened by incorporation of selective removal devices into the crystallizer operation. For example, one can add a fines destruction unit so that fines may be advanced or redissolved and returned to the crystallizer. If the flow rate of liquor containing fines is (R - 1) times the output flow rate, then the removal rate of fines below a cut size L_F is R times the removal rate of larger crystals. The crystal size distribution for this system is given by:

$$n = n_F^o \exp(-RL/G\tau);\ L \le L_F \qquad \text{[II.6]}$$

$$n = n^o \exp(-L/G\tau);\ L \ge L_F \qquad \text{[II.7]}$$

Since these two equations intersect, n° is related easily to n°_F, G, and R. Analysis of these equations shows that fines destruction leads to an increase in dominant crystal size and spread of the distribution.

Alternatively, with a coarse product removal system one can remove crystals above size L_C from the crystallizer at a rate "z" times the removal rate of smaller crystals. Under such conditions, the crystal size distribution may be written as

$$n = n^o \exp(-L/G\tau);\ L \le L_C \qquad \text{[II.8]}$$

$$n = n^o \exp(-zL/G\tau);\ L \ge L_C \qquad \text{[II.9]}$$

The product will exhibit a narrower size distribution with a concomitant reduction in dominant size.

Finally, if we remove both fines and large crystals, the size distribution is given by:

$$n = n_F^o \exp(-RL/G\tau);\ L \le L_F \qquad \text{[II.10]}$$

$$n = n^o \exp(-L/G\tau);\ L_F \le L \le L_C \qquad \text{[II.11]}$$

$$n = n^o \exp(-zL/G\tau);\ L_C \le L \qquad \text{[II.12]}$$

Generally, operation with both of these selective removal functions combines the best features of each: namely, increased dominant size and narrower distribution. Figure II.5 illustrates a typical crystal size distribution plot taken from the well-mixed region of

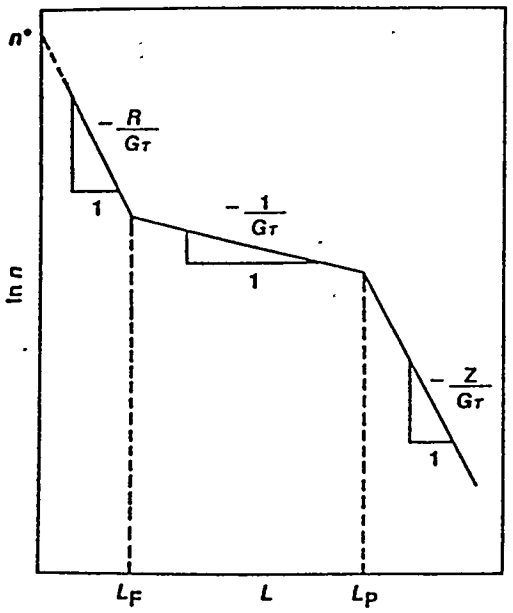

Figure II.5. Crystal size distribution with combined fines and coarse product removal (reference II.2).

a crystallizer having both fines and course selective removal devices. The agreement of theory and the experimental prediction is illustrated in Figure II.6.

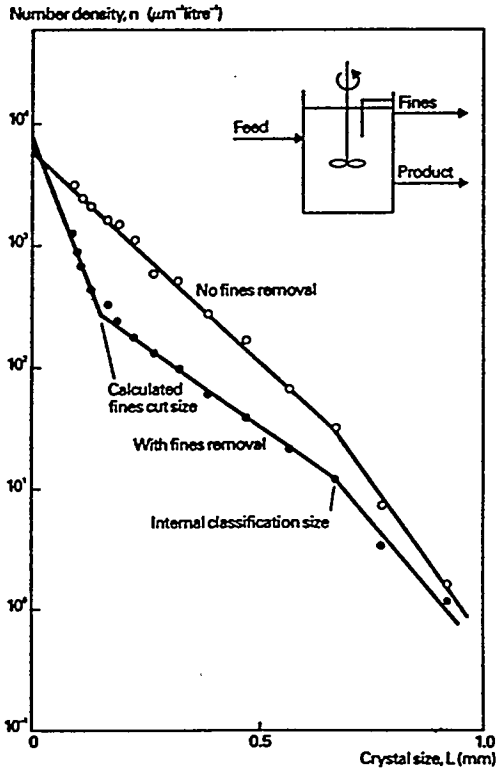

Figure II.6. Effect of size-dependent residence time on the crystal size distribution of potassium nitrate in a continuous crystallizer (reference II.5).

The analogy between the data in Figure II.6 for potassium nitrate crystallization (II.4) and a typical ASF plot for the FTS products from a continuous stirred tank reactor (CSTR) is obvious (Figure II.7, Ref. II.6).

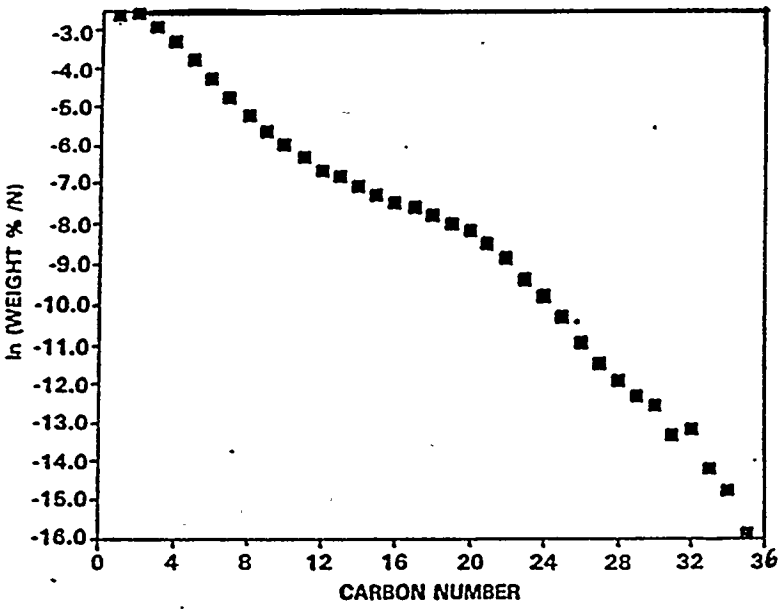

Figure II.7. Anderson-Schulz-Flory plot of products after ca. 60 days of syngas conversion (reference II.6).

If there is a connection between the two sets of data, the reason for the first alpha plot would be that gaseous products are removed rapidly from the reactor because of their volatility and that heavier products are removed from further growth because of their limited solubility. The two- or multi-alpha ASF plots are considered in more detail in a later section.

Precipitation of hydroxides is a more complex process since chemical reactions (e.g., elimination of water, conversion of basic salts into hydroxides) also occur during formation of the solid phase, depending on the pH value and time. Consequently, there are as yet very few theoretical schemes for the general treatment of the precipitation of hydroxides.

II.A.2. Nucleation

The formation of submicroscopic particles (nuclei) of the new phase from a supersaturated solution is particularly interesting, but relatively difficult to observe experimentally. It generally begins only when a certain supersaturation has been reached, and then proceeds very rapidly. The questions that arise in connection with the formation of a new phase have already been considered in detail by, among others, Tammann (II.7), Ostwald (II.8) and Volmer (II.9). The kinetics of precipitation reactions have also been described by Nielsen (II.10) and Lieser (II.11.). The following discussion draws heavily upon references II.10 and II.11 and in sections directly quoted from one of these references.

Lieser writes (II.11): "Nucleation can be either homogeneous (spontaneous) or heterogeneous. Homogeneous or spontaneous nucleation occurs without the participating of other substances, by combination of the dissolved ions or molecules to form larger particles. Heterogeneous nucleation begins on small particles of foreign matter (seeds), on which ions or molecules are deposited (e.g., by adsorption) until a nucleus has been formed."

"Relatively high supersaturations are often observed in the absence of seeds. The supersaturation S is defined by

$$S = \frac{C - C_s}{C_s} \qquad \text{[II.13]}$$

The ratio $C/C_s = S + 1 = S'$ is known as the supersaturation ratio. C is the actual concentration and C_s is the saturation concentration (solubility). The occurrence of supersaturation can be explained thermodynamically by means of the surface tension.

The change in free enthalpy ΔG is given by the difference in the chemical potentials μ of the substance in question per molecule in the dissolved (μ_1) and in the solid (μ_2) state and by the surface tension σ:

$$\Delta G = -n(\mu_1 - \mu_2) + \sigma F \qquad \text{[II.14]}$$

n is the number of molecules in a nucleus. If the nuclei are assumed to be spherical, then $F = n^{2/3} f$ [$f = (3v)^{2/3} (4\pi)^{1/3}$; v = volume of a molecule] and

$$\Delta G = -n(\mu_1 - \mu_2) + n^{2/3} f\sigma \qquad \text{[II.15]}$$

The curve in Figure II.8 shows ΔG as a function of the number of molecules in a nucleus. For small values of n, ΔG is always positive, i.e., very small nuclei redissolve. A metastable equilibrium exists at the maximum of the curve (d ΔG/dn = 0); this corresponds to the critical state for nucleation (denoted hereafter by an asterisk)."

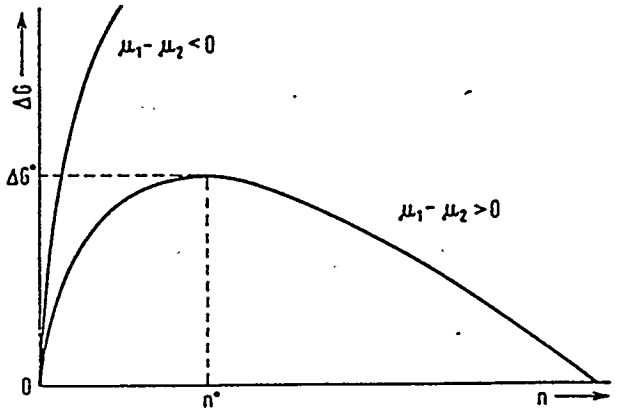

Figure II.8. Free enthalpy ΔG as a function of the number of molecules n in a nucleus (n* = number of molecules in a critical nucleus) (reference II.11).

"A nucleus in which the number of molecules n = n* is known as a critical nucleus, and particles in which the number of molecules n < n* are called subnuclei

or embryos. Whereas all nuclei having n < n* redissolve, nuclei with n > n* grow into crystals. A homogeneously supersaturated solution is therefore thermodynamically in a metastable state, which can persist for a very long time. A precipitate can form only when the energy barrier ΔG^* has been overcome; in homogeneous nucleation, for example, this can occur as a result of random free enthalpy variations in small regions of the solution."

"Information about the radius of a critical nucleus and the number of molecules that it contains can be obtained from the following argument. For spherical particles,

$$F = \frac{3V}{r} \quad . \qquad \text{[II.16]}$$

Since dV/dn = v (volume of one molecule), it follows from eq. [II.14] that

$$\frac{d\Delta G}{dn} = -(\mu_1 - \mu_2) + \frac{2v\sigma}{r} \quad . \qquad \text{[II.17]}$$

In the metastable equilibrium, d ΔG/dn = 0, and the radius of the critical nucleus is therefore

$$r^* = \frac{2v\sigma}{\mu_1 - \mu_2} \quad . \qquad \text{[II.18]}$$

The number of molecules in a critical nucleus is

$$n^* = \frac{V^*}{v} = \frac{2\sigma F^*}{3(\mu_1 - \mu_2)} \quad . \qquad \text{[II.19]}$$

The free enthalpy of the critical nucleus is

$$\Delta G^* = -n^*(\mu_1 - \mu_2) + \sigma F^* \quad .$$

The surface area F* of the critical nucleus is found with the aid of eq. [II.19] to be

$$\Delta G^* = -\frac{2\sigma F^*}{3} + \sigma F^* = \frac{\sigma F^*}{3} \quad . \qquad \text{[II.20]}$$

$$F^* = 3\beta \frac{\sigma^2 v^2}{(\mu_1 - \mu_2)^2} \quad . \qquad \text{[II.21]}$$

where β is a geometric shape factor:

$$\beta = \frac{4F^3}{27V^2} \quad . \qquad \text{[II.22]}$$

[β = 16.76 (sphere), 20.22 (icosahedron), 22.20 (dodecahedron), 27.71 (octahedron), 32 (cube), 55.43 (tetrahedron)]."

"The difference in the chemical potentials is given by the ratio of the activities a in the solution (a_1) and in the solid (a_2):

$$\mu_1 - \mu_2 = kT \ln \frac{a_1}{a_2} \qquad \text{[II.23]}$$

If the concentration and saturation concentration are used as approximations for the activities, it follows, with the aid of eq. [II.1], that

$$\mu_1 - \mu_2 = kT \ln(S + 1) \qquad \text{[II.24]}$$

and from equations [II.19], [II.21], and [II.24]:

$$n^* = 2\beta \frac{\sigma^3 v^2}{[kT \ln(S^* + 1)]^3} \qquad \text{[II.25]}$$

S* = critical supersaturation.

"Equation [II.25] permits the rough calculation of the number of molecules in a critical nucleus. Measured values for the surface tension σ are available in only a few

cases; it is of the order of 100 erg/cm^2. From σ and the critical supersaturation S*, we obtain n* values of the order of 100, i.e., a critical nucleus consists of about 100 molecules and has a diameter of the order of 100 Å."

"The radius of a nucleus in a supersaturated solution is given by the Gibbs-Kelvin equation (reference II.12)

$$r = \frac{2v\sigma}{kT\ ln(S + 1)} \qquad [II.26]$$

which follows from equations [II.18] and [II.24]. According to this equation at a certain supersaturation S, only particles of one particular size are present in the solution, this size decreasing with increasing supersaturation (Figure II.9)."

"The calculation provides no details on the concentration of subnuclei in a supersaturated solution, which is very strongly dependent on the supersaturation (Figure II.10). The number of critical nuclei also changes extremely rapidly with the supersaturation, so that S* can be determined relatively accurately by experiment. Slightly below this critical supersaturation, the number of critical nuclei is still very small

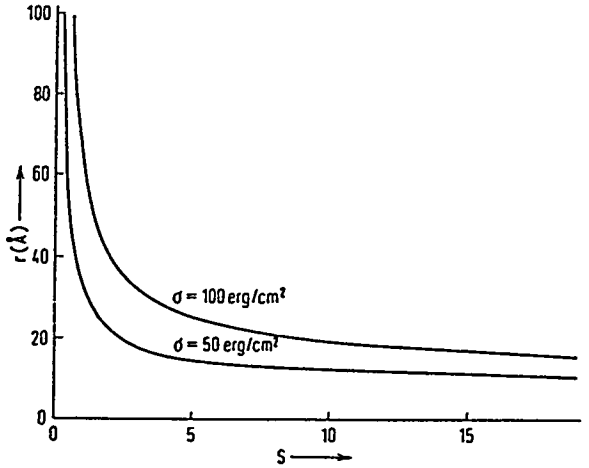

Figure II.9. Radius of the nuclei in a supersaturated solution as a function of the supersaturation S on the basis of the Gibbs-Kelvin equation for various surface tensions (reference II.11).

(i.e., the nucleation rate is very low), whereas only slightly above the critical supersaturation the number of critical nuclei is so large that precipitation begins almost instantaneously."

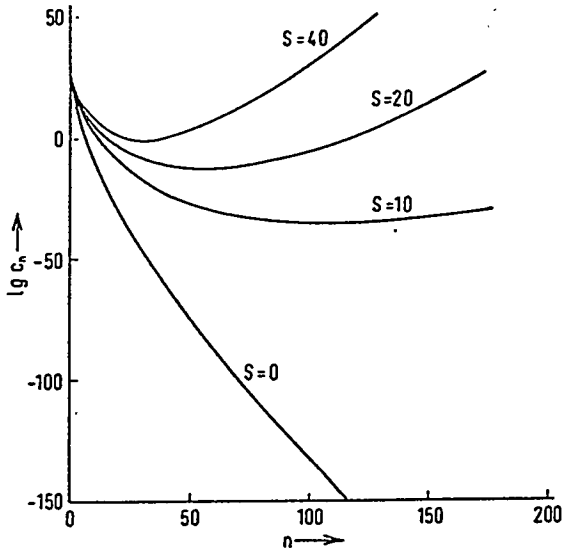

Figure II.10. Concentration of subnuclei in a supersaturated solution on the basis of theoretical considerations (n = number of molecules in a subnucleus, S = supersaturation; calculated for $\beta = 40$, $\sigma = 50$ erg/cm^2, v = 10^{-22}cm^3, $C_s = 2.5 \times 10^{-6}$ mole $\cdot$ 1^{-1}) after Nielsen (II.10).

"The first equation for the nucleation rate was given by Volmer and Weber (II.13), and later by Becker and Döring (II.14); further theoretical treatments were given by Nielsen (II.10) and Kahlweit (II.15). The nucleation rate J (number of nuclei formed per cm^3 per sec) can be expressed by

$$J = J_0 \exp[-\Delta G^*/kT] \qquad \text{[II.27]}$$

It follows with the aid of equations [II.20], [II.21], and [II.24] that

$$\log J = \log J_0 - \frac{A}{[\log (S + 1)]^2} \qquad \text{[II.28]}$$

where

$$A = \frac{\beta \sigma^3 v^2}{(kT \ ln \ 10)^3} \qquad \text{[II.29]}$$

as an approximation

$$\log J \approx 30 - \frac{A}{[\log (S + 1)]^2} \qquad \text{[II.30]}$$

The nucleation rate according to this equation can be found from a diagram (Figure II.11; reference II.10). For spontaneous (homogeneous) nucleation, the experimental values of J as a function of the supersaturation S lie on a curve having a constant value for A; it is therefore possible to calculate the surface tension σ with the aid of eq. [II.29]."

"Figure II.11 shows that the nucleation rate for relatively wide ranges can be approximately given by a relation of the form

$$J = k_m C^m \qquad \text{[II.31]}$$

The exponent m corresponds to the slope d (log J)/d (log c) of the experimental curve, and also provides information about the size of a critical nucleus; it is found from equations [II.28] and [II.25] that

$$\frac{d \log J}{d \log c} = m = \frac{d \ ln \ J}{d \ ln \ (S + 1)} = \frac{2\beta \sigma^3 v^2}{[kT]^3 [ln(S + 1)]^3} = n^* \qquad \text{[II.32]}$$

The surface tension can finally also be determined with the aid of this equation."

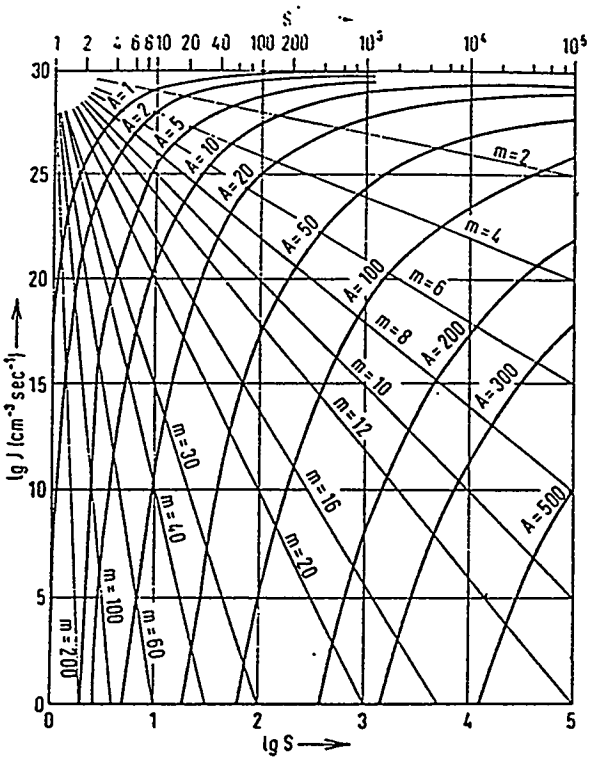

Figure II.11. Nucleation rate (number of nuclei formed per cm^3sec^{-1}) as a function of the supersaturation for various values of A (eq. [II.28] and reference II.10).

II.A.3. Growth

Once a critical nucleus has been formed, it can grow into a crystal in various ways. The first detailed theoretical treatment of crystal growth was due to Kossel (II.16) and Stranski (II.17); the basic model is shown schematically in Figure II.12.

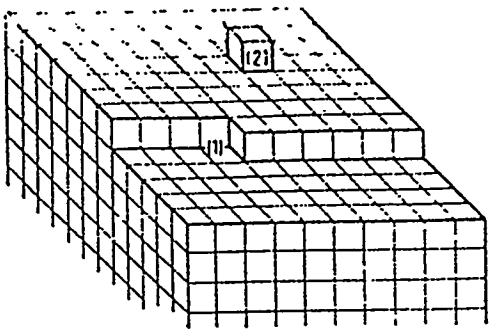

Figure II.12. Model of crystal growth according to Kossel (II.16) and Stranski (II.17).

"According to this model of stepwise growth, there are non-equivalent sites on the surface of a crystal. A site marked (1) in figure II.13 is preferred, while the edges and corners of the crystal are less favorable. The first step in the formation of a new layer has particularly unfavorable energy requirements. The particle (2), which is a surface nucleus, forms a new layer by two-dimensional growth. It is also possible that more than one surface nucleus is deposited, and in this case the zones formed by the two-dimensional growth of these nuclei overlap. If the formation of surface nuclei is very fast, a new layer is started before the growth of the last layer is complete, i.e., the (polynuclear) growth takes place in several layers simultaneously one upon another (Figure II.13)."

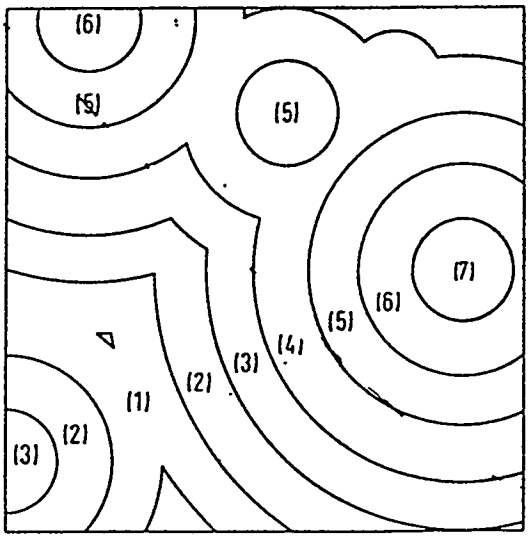

Figure II.13. Polynuclear growth (schematic; the numbers denote superimposed layers) (reference II.10).

"As an alternative to stepwise growth, Frank (II.18) proposed growth on screw dislocations (Figure II.14), where there are always energetically favorable sites for the

deposition of ions or molecules. The screw dislocation is retained as a crystal imperfection, and is continuously propagated in the form of a spiral as growth

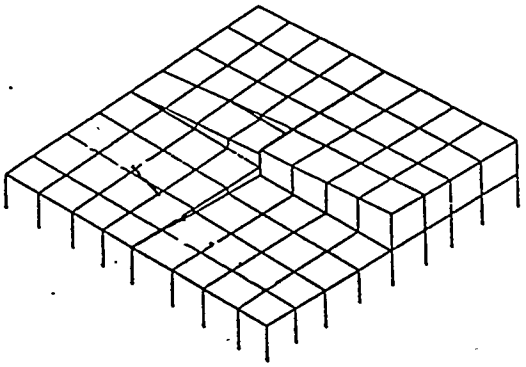

Figure II.14. Growth at screw dislocations.

proceeds. The formation of surface nuclei is no longer necessary, and growth at screw dislocations can therefore occur even at low supersaturations. In agreement with this model, spiral growth at screw dislocations has in fact been observed in many cases."

"Various consecutive processes may be important to the crystal growth: (a) diffusion of the ions or molecules from the solution onto the surface; (b) adsorption of the ions or molecules on the surface; (c) transition on the surface; (d) transport on the surface to a suitable site." Process (b) is very much faster than the other processes, since it is not inhibited. The processes (c) and (d) are generally indistinguishable, and are therefore known collectively as the surface reaction. The rate-determining step for the growth of the crystals may thus be the diffusion or the surface reaction."

"If the diffusion is rate-determining, the growth rate of a crystal is given by

$$\frac{dn}{dt} = 4\pi D(C - C_s)r \qquad \text{[II.33]}$$

This yields the relation given by Neumann (II.19) for the radius of a particle as a function of time:

$$r(t) = \sqrt{2DV(C-C_s)t} \qquad \text{[II.34]}$$

V is the molar volume and D is the diffusion coefficient. Eq. [II.34] is valid only when V ($C-C_s$) << 1. If on the other hand the surface reaction is rate-determining, it may be assumed that the growth rate of a crystal is proportional to the area and to the concentration difference (II.15), and one then obtains

$$\frac{dn}{dt} = 4\pi r^2 k(C-C_s) \qquad \text{[II.35]}$$

and

$$r(t) = kV(C-C_s)t \qquad \text{[II.36]}$$

Equations [II.33] to [II.36] are applicable provided that the linear growth of a crystal can be followed as a function of time. If growth and ripening overlap, as is usually the case in the precipitation of sparingly soluble ionic crystals, dn/dt and dr/dt may be positive or negative for a given crystal."

"In many cases we are interested in the decrease in concentration in the solution as a result of crystal growth, which can be described by a kinetic equation

$$J = -\frac{dn_L}{dt} = k_m C^m \qquad \text{[II.37]}$$

n_L is the number of ions or molecules per cm^3 of solution. However, Marc (II.20) showed that the growth rate for readily and moderately soluble substances satisfies the equation

$$J = k_m(C - C_s)^m \qquad \text{[II.38]}$$

The exponent **m** is usually known as the order of the growth reaction. This is correct in the sense used in chemical kinetics for a relation of the form of eq. [II.37], but not for an empirical relation of the type of eq. [II.38]."

"The progress of crystal growth can also be described by the change in the supersaturation; the characteristic quantity used (II.10) is

$$\alpha = 1 - \frac{S}{S_o} \qquad \text{[II.39]}$$

S_o is the supersaturation at time t = 0. For spherical particles of (average) radius **r** and a constant number of particles,

$$r = r_e \alpha^{1/3} \qquad \text{[II.40]}$$

r_e is the (average) radius of the crystals at the end of the experiment. For the case where diffusion is rate-determining, Nielsen (II.10) derived from this relation

$$t = K_D I_D \qquad \text{[II.41]}$$

where

$$K_D = \frac{r_e^2}{3VD(C_o - C_s)} \qquad [II.42]$$

and I_D is the "diffusion chronomal"

$$I_D = \int_0^{\alpha} \frac{dx}{x^{1/3}(1-x)} \qquad [II.43]$$

Figure II.15 shows α as a function of I_D. This diagram can be used for the evaluation of measurements, e.g., by reading off I_D for the experimental value of α and plotting it as a function of time. If the diffusion is rate-determining, as was assumed in the derivation of eq. [II.41], this procedure should give a straight line, the slope of which $(1/K_D)$ should, according to eq. [II.42], give reasonable values for the diffusion coefficient D. For aqueous electrolytes, D is of the order of 10^{-5} cm^2 sec^{-1} at room temperature."

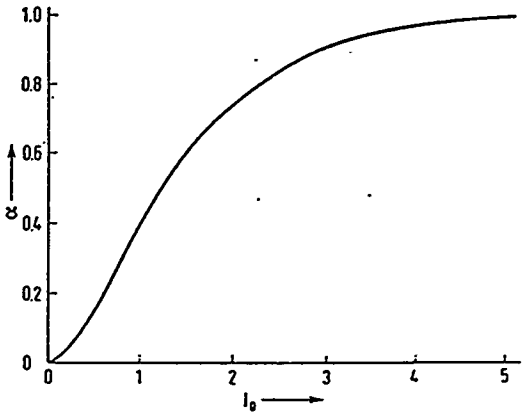

Figure II.15. Diffusion chronomal after Nielsen (II.10) (eq. [II.39] to [II.43]).

"For the case in which the surface reaction is rate-determining, Nielsen (II.10) uses the quantity

$$\alpha = 1 - \frac{C}{C_o} \qquad \text{[II.44]}$$

and with the aid of eq. [II.40] he obtains the following relations for mononuclear or polynuclear growth."

$$t = K_m I_m \text{ and } t = K_p I_p \qquad \text{[II.45]}$$

II.A.4. Ripening

Crystals formed by nucleation and growth are usually imperfect. These crystals are not at thermodynamic equilibrium with the solution, and the deviation increases with increasing supersaturation of the solution. Thus, the increasing rate of formation of small crystals with increasing supersaturation increases the deviation from thermodynamic equilibrium.

"According to Ostwald (II.8), small crystals pass into solution during ripening, while the larger crystals continue to grow (Ostwald ripening). Another theory (II.21) involves the combination of small particles and growth of the resulting composite particles into larger crystals (cementation) (II.11)."

"If we consider the Ostwald ripening mechanism, only some of the crystals formed in any stage of a precipitation reaction have a chance to grow further. The remaining crystals redissolve. This is true in particular during the growth stage, since the supersaturation in the solution often changes very markedly in this stage."

"The rate of Ostwald ripening is subject to the same considerations as the rate of growth of the crystals. The ripening may be divided into the following processes: (a) dissolution of ions or molecules from small crystals, (b) diffusion of the dissolved